NeuroImage: Clinical 38 (2023) 103371

Contents lists available at ScienceDirect

NeuroImage: Clinical

journal homepage: www.elsevier.com/locate/ynicl

# Longitudinal changes in surface based brain morphometry measures in amnestic mild cognitive impairment and Alzheimer's Disease

Tobias Bachmann [a,1,*], Matthias L. Schroeter [b,c], Kewei Chen [d,f,g,h], Eric M. Reiman [d,e,f,h,i], Christopher M. Weise [a,j], for the Alzheimer's Disease Neuroimaging Initiative

[a] University of Leipzig Medical Center, Department of Neurology, Germany
[b] Max Planck Institute for Human Cognitive and Brain Sciences, Department of Neurology, Leipzig, Germany
[c] Clinic of Cognitive Neurology, University Hospital Leipzig, Leipzig, Germany
[d] Banner Alzheimer's Institute, Phoenix, AZ, USA
[f] Arizona Alzheimer's Consortium, Phoenix, AZ, USA
[g] School of Mathematics and Statistics (KC), Neurodegenerative Disease Research Center (EMR), Arizona State University, USA
[h] Department of Neurology, College of Medicine – Phoenix (KC), Department of Psychiatry (EMR), University of Arizona, USA
[e] Neurogenomics Division, Translational Genomics Research Institute, University of Arizona, and Arizona State University, Phoenix, AZ, USA
[i] Banner-Arizona State University Neurodegenerative Disease Research Center, BioDesign Institute, Arizona State, University, Tempe, AZ, USA
[j] University of Halle Medical Center, Department of Neurology, Germany

A B S T R A C T

*Background:* Alzheimer's disease (AD) is associated with marked brain atrophy. While commonly used structural MRI imaging methods do not account for the complexity of human brain morphology, little is known about the longitudinal changes of cortical geometry and their relationship with cognitive decline in subjects with AD.

*Methods:* Data from the Alzheimer's Disease Neuroimaging Initiative (ADNI) were used to perform two-sample t-tests to investigate longitudinal changes of cortical thickness (CTh) and three surface-based morphometry measures: fractal dimension (i.e. cortical complexity; FD), gyrification index (GI), and sulcal depth (SD) in subjects with AD, amnestic mild cognitive impairment (aMCI) in comparison to cognitively unimpaired controls (CU) in baseline and 2-year follow-up sMRI scans. In addition, correlations of the morphological measures with two-year cognitive decline as assessed by the modified AD Assessment Scale-Cognitive Subscale (ADAS-Cog 11) were calculated via regression analyses.

*Results:* Compared to CU, both AD and aMCI showed marked decreases in CTh. In contrast, analyses of FD and GI yielded a more nuanced decline of the respective measures with some areas showing increases in FD and GI. Overall changes in FD and GI were more pronounced in AD as compared to aMCI. Analyses of SD yielded widespread decreases. Interestingly, cognitive decline corresponded well with CTh declines in aMCI but not AD, whereas changes in FD corresponded with AD only but not aMCI, whereas GI and SD were associated with cognitive decline in aMCI and AD.

*Conclusion:* Patterns of longitudinal changes in FD, GI and SD were only partially overlapping with CTh reductions. In AD, surface-based morphometry measures for brain-surface complexity showed better correspondence than CTh with cognitive decline over a two-year period of time. Being drawn from measures reflecting changes in more intricate aspects of human brain morphology, these data provide new insight into the complexity of AD-related brain atrophy and its relationship with cognitive decline.

## 1. Introduction

Dementia is estimated to affect over 50 million people worldwide. Of these cases, >50% are attributable to Alzheimer's Disease (AD) (Prince et al., 2014) making AD the most common neurodegenerative disease. Neurobiologically it is characterized by the extracellular accumulation of Amyloid ß 1–42 and intracellular aggregates of phosphorylated Tau-protein (i.e. neurofibrillary tangles). In the majority of cases, sporadic late-onset AD is clinically characterized by progressive cognitive decline, most prominently in mnestic functions in early stages.

In the past decades, a number of imaging biomarkers have been established and proven helpful in the diagnosis of AD and the tracking of

* Corresponding author at: University of Leipzig, Department of Neurology, Liebigstr. 20, 04103 Leipzig, Germany.
*E-mail address:* tobias.bachmann@medizin.uni-leipzig.de (T. Bachmann).

[1] Data used in preparation of this article were obtained from the Alzheimer's Disease Neuroimaging Initiative (ADNI) database (adni.loni.usc.edu). As such, the investigators within the ADNI contributed to the design and implementation of ADNI and/or provided data but did not participate in analysis or writing of this report. A complete listing of ADNI investigators can be found at http://adni.loni.usc.edu/wp-content/uploads/how_to_apply/ADNI_Acknowledgement_List.pdf.

https://doi.org/10.1016/j.nicl.2023.103371
Received 4 August 2022; Received in revised form 14 December 2022; Accepted 6 March 2023
Available online 8 March 2023

its progression (de Leon et al., 1997; Femminella et al., 2018; Park and Moon, 2016; Zhang and Liu, 2018), with structural MRI (sMRI) being the most extensively used and studied method. Here, specific patterns of atrophy can be observed that have been shown to correspond to AD-related cognitive decline in both cross-sectional and longitudinal studies. Typically, regional atrophy can be observed early within medial temporal structures including the hippocampus, but as the disease progresses, atrophy expands to the lateral temporal cortex, precuneus, posterior cingulate cortex and further parietal and frontal cortical regions become affected (Baxter et al., 2006; Bejanin et al., 2017; Dubois et al., 2010; Gordon et al., 2018; McKhann et al., 2011; Risacher et al., 2017; Schroeter et al., 2009; Whitwell et al., 2012).

Common methods used to study brain morphological changes related to AD include voxel-based morphometry, cortical thickness and regional measure-based (such as ROI) volumetric measures. Nevertheless, commonly applied sMRI-based imaging methods and biomarkers (e.g. hippocampal volume or cortical thickness) do not fully account for the complexity of human brain morphology, which – next to volumetric aspects of the cerebral cortex – also encompasses the architecture and shape of its surface structures such as gyri and sulci. Compared to the amount of purely volumetric studies, relatively little is known on how surface morphological brain features are affected by AD, particularly with respect to their changes over time and how they relate to cognitive function. Previous studies successfully employed surface-based morphometry (SBM) measures in AD research. While some were purely cross-sectional and focused on individual measures (King et al., 2010; Nicastro et al., 2020; Ruiz de Miras et al., 2017), most longitudinal studies were either ROI-based (Li et al., 2022; Wu et al., 2021) or otherwise constrained to specific brain regions (Dong et al., 2020). We found one previous whole-brain longitudinal SBM study, which used SBM to build a machine-learning classifier to distinguish AD from MCI and CU individuals and was not concerned with a comparison of different measures and their reflecting of cognitive decline (Qin et al., 2022). Thereforewe aimed to investigate whole-brain longitudinal changes of different SBM measures (Dale et al., 1999; Fischl et al., 1999; Fischl and Dale, 2000) able to capture different aspects of brain morphology and their relationship with cognitive decline in subjects with AD and subjects at high risk for AD (i.e. amnestic mild cognitive impairment, aMCI) in comparison to cognitively unimpaired controls (CU) and compare these measures with longitudinal changes of cortical thickness (CTh), a commonly applied measure of brain atrophy.

## 2. Methods

### 2.1. Participants

Data used in the preparation of this article were obtained from the Alzheimer's Disease Neuroimaging Initiative (ADNI) database (adni.loni.usc.edu). The ADNI was launched in 2003 as a public–private partnership, led by Principal Investigator Michael W. Weiner, MD. The primary goal of ADNI has been to test whether serial magnetic resonance imaging (MRI), positron emission tomography (PET), other biological markers, and clinical and neuropsychological assessment can be combined to measure the progression of mild cognitive impairment (MCI) and early Alzheimer's disease (AD). Classification of subjects as CU, suffering from aMCI or AD was based on performance in the Mini-Mental State Examination (MMSE; Folstein et al., 1975), Clinical Dementia Rating (CDR) scale (Hughes et al., 1982) and Logical Memory II subscale of the Wechsler Memory Scale–Revised (Petersen et al., 2010). For up-to-date information and information regarding subject recruitment, inclusion and exclusion criteria see https://www.adni-info.org. The ADNI employs a standardized protocol for acquiring and preprocessing MRI data. All image series undergo manual quality control for protocol adherence and scan quality by trained personnel. Here, as recommended by the ADNI investigators, we made use of a standardized and uniformly pre-processed MRI data collection provided by ADNI (i.e. ADNI1: Complete 2Yr 1.5 T), comprising structural 3-dimensional MPRAGE data from a total of n = 479 subjects (Wyman, 2013).

### 2.2. Preprocessing

All neuroimaging MR data were processed and analyzed with the Computational Anatomy Toolbox (CAT12; https://www.neuro.uni-jena.de/cat) and Statistical Parametric Mapping (SPM12; Wellcome Department of Cognitive Neurology). CAT12′s longitudinal preprocessing pipelines were used with default settings and surface and thickness estimation was applied to structural MR images. Detailed description of the individual preprocessing steps can be found in the CAT12 Manual (Gaser and Dahnke, n.d.). In brief, baseline and follow-up images were co-registered for each individual and then realigned across the entire sample. The preprocessing pipeline further included bias correction, image segmentation (i.e. into cerebrospinal fluid, white matter and gray matter), transformation into MNI space and DARTEL normalization. Specific SBM methodological aspects are listed below. Finally, data were smoothed with a 15-mm (for cTH) or a 25-mm (for FD, GI, SD) FWHM Gaussian kernel, and delta images (i.e. "follow-up" minus "baseline") were created via CAT 12′s cat_stat_diff function.

### 2.3. SBM measures

SBM uses vertices instead of voxels to explicitly capture aspects of the brain's surface, in particular the shape of its sulci and gyri. Four different SBM measures were used. While we provide a detailed discussion of the respective SBM measures' merit and rationale in the following paragraphs, this short overview can serve as an orientation: (a) Cortical thickness (CTh) estimates cortical thickness and therefore gray matter mass (Dahnke et al., 2013). (b) Gyrification index (GI) relates an idealized smooth surface of the brain, i.e. its hull, to its sulci's contour, thereby providing a compact quantification of folding complexity. In the form used here, local GI, it allows for an area-wise inter-subject comparison of gyrification levels (Luders et al., 2006). (c) Sulcal depth (SD) describes the geographical depth of sulcal folds by measuring the maximum distance of any given fold to, again, an outer hull (Dahnke et al., 2013; Gaser and Dahnke, n.d.). (d) Fractal dimension (FD) is an intrinsic measure of cortical complexity. It takes advantage of the brain being approximately a fractal object, i.e. consisting of self-similar components, summarizing details over a range of scales (Yotter et al., 2011).

We opted for SBM as a vertex-based approach as this method allows not only to investigate AD-related loss of brain matter (via CTh), but also different aspects of brain atrophy, such as reductions in cortical complexity/folding. Considering the importance of folding for increasing cortical surface and therefore gray matter, the combination of different SBM measures may provide more comprehensive information on the macrostructural changes associated with neurodegenerative diseases such as AD as compared to other commonly applied methods such as voxel-based morphometry (VBM). In particular, and among other problems, VBM suffers from partial volume effects when it comes to assessing cortical surface features. Two voxels in two separate gyri separated by a sulcus might seem geographically close in the folded brain and may be considered as such by VBM due to a lack of surface recognition, while they are actually, were the brain unfolded, geographically and, of more interest to research, functionally distant (Acosta et al., 2009; Clarkson et al., 2011; Lerch and Evans, 2005). In addition to the more commonly used CTh, we employed FD, GI, and SD to estimate longitudinal changes in cortical morphology. Loss of gray matter – regional in early stages and more globally in later stages - are the most striking brain morphological feature of AD (Karas et al., 2004).

In the realm of surface-based methods, gray matter mass is conceptualized as CTh. Methods of CTh estimation are based on separating gray matter rom white matter and cerebrospinal fluid, which is a significant challenge given the highly convoluted nature of the brain's surface.

They differ in their consideration of partial volume effects, with the simplest methods tending to overestimate CTh due to inaccurate modeling of sulci, while more sophisticated methods of sulci reconstruction tend to be prohibitively computationally intensive. In CAT12 this dilemma is solved by implementing the projection-based thickness method, a fully automated, yet reliable (even in non-standard brains) approach, which focuses on the distance of gray matter voxels to white matter voxels as opposed to the distance of gray matter to cerebrospinal fluid voxels, on account of the former being less prone to partial volume effects. On the gray matter's outer border, the distance to white matter reaches its local maximum, which is then simply projected inwards, thus reconstructing the cortical surface (Dahnke et al., 2013).

While CTh measures have to abstract from folding patterns, we used three different methods of capturing this important aspect of brain morphology. Brain disorders have been shown to manifest in characteristic variations of brain surface variability. Gyrification patterns, for example, are a sensitive structural neuroimaging marker of brain disorders. One of its oldest and most widely used reproducible and standardized metrics, GI, is defined as the ratio of the inner contour, following the sulcal folds, to the outer contour, i.e. a virtual hull covering the brain's surface (Zilles et al., 1988). It has been shown to be specifically altered in various neurological disorders (Libero et al., 2019; Matsuda and Ohi, 2018; Sterling et al., 2016) and to correspond to functional alterations (Schaer et al., 2013). In CAT12, GI is implemented in the form of a multitude of local GI (as opposed to a single global GI) comprehensively covering the entire brain surface (Luders et al., 2006).

SD, on the other hand, measures the straight-line distance between the central surface (i.e. half-way between the gray matterto white matter border and the gray matter to cerebrospinal fluid border) and, likewise, an outer hull (Dahnke et al., 2013; Gaser and Dahnke, n.d.).

Being reliant on constructing an external idealized contour, both GI and SD can be considered extrinsic metrics of cortical complexity. In contrast, FD aims to be an intrinsic measure. It is based on the notion of the brain being, to a certain extent, a fractal object. Besides forgoing external assumptions, CAT12′s implementation of FD calculation is able to estimate FD values for each vertex in each subject's brain, avoiding the need for (a) exceedingly accurate inter-subject alignments and (b) multiple downsampling and, consequently, reconstructing surfaces, which introduces inaccuracies (Yotter et al., 2011). Thus, FD allows for a compact, reliable, and informative assessment of cortical complexity on a within-subject and inter-subject level. Previous research has demonstrated significant differences in FD in a number of brain disorders, including AD (Ha et al., 2005; King et al., 2010, 2009).

### 2.4. Data analyses

CAT12 and SPM12 were used to investigate longitudinal within-group and inter-group differences of SBM measures. To do so, we applied two-sample t-tests on our delta images. To investigate associations of brain morphological changes with cognitive changes, we

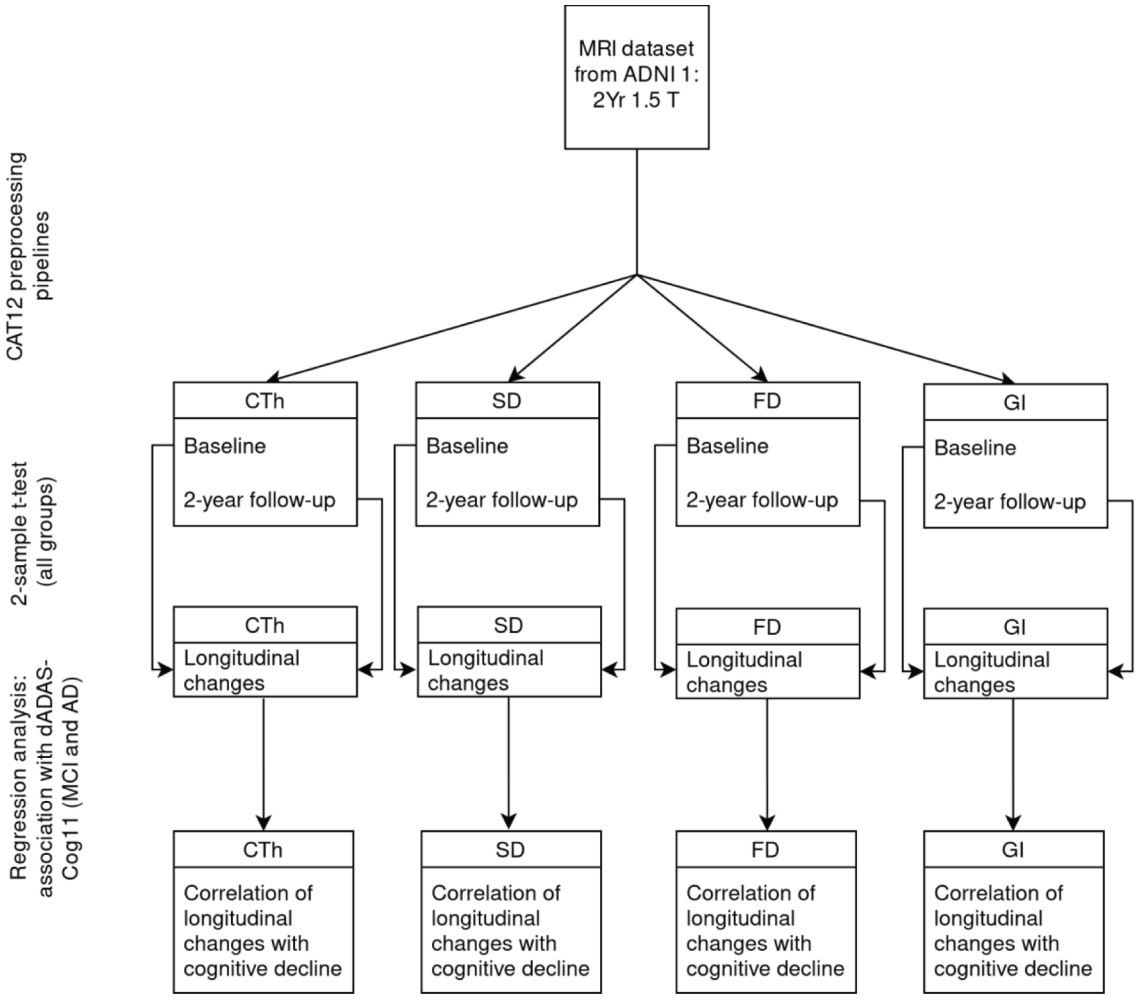


**Fig. 1.** Flowchart illustrating our approach. AD: Alzheimer's disease. AMCI: amnestic mild cognitive impairment. CTh: Cortical thickness. SD: Sulcal depth. GI: Gyrification index. FD: fractal dimension.

performed multiple regression analyses with delta AD Assessment Scale-Cognitive Subscale (ADAS-cog 11) values as variables of interest (see Fig. 1 for a flowchart depicting our analysis approach). SPM12′s ANOVA implementation was used for additional post-hoc interaction analyses (i.e. group*cognitive decline). All our models contained corrections for age and sex since they were specified as covariates in our analyses. Significance was determined via the threshold-free cluster enhancement (TFCE) method (Smith and Nichols, 2009), which allows for cluster-based inference without the need to pre-specify arbitrary thresholds. Its implementation in the TFCE toolbox for CAT12 performs non-parametric permutation tests, thus avoiding problems inherent to parametric statistics (Eklund et al., 2016). Family-wise error (FWE) correction was applied with respect to the entire brain and we considered a corrected $p < 0.05$ as significant. Labeling of significant clusters was done with GingerALE (https://brainmap.org/software.html) and the Talairach Client (https://talairach.org/client.html). Non-imaging statistical analyses were carried out with SAS Software (SAS Institute Inc., version 9.4, Cary, NC) and R 4.0.0 (R Core Team, 2020).

## 3. Results

Participant characteristics are summarized in Table 1. Our samples consisted of 96 subjects with AD (75.2y ± 7.4), 211 subjects with aMCI (74.8y ± 7.0), and 165 CU (76y ± 4.9) controls. Of these subjects, we used baseline and 2-year follow-up (mean follow-up time 741 ± 33 days) sMRI scans and, as a measure of cognitive decline over time, corresponding modified ADAS-Cog 11 values (Rosen, 1984). Expectedly, a higher frequency of the APOE e4 risk allele was observed in both AD and aMCI participants in comparison to CU, as well as in AD vs. aMCI participants. Cognitive performance as measured by the ADAS11 and MMSE differed significantly between the groups and declined significantly in AD and aMCI subjects (AD > MCI). No significant group differences were found for age and follow-up time, however sex was not completely balanced between groups ($p = 0.002$). Note that we corrected systematically for sex (and age) in the following analyses controlling for a potential bias here.

Of 211 aMCI subjects, 85 converted to AD within the 2-year timeframe between baseline and follow-up. No significant age or sex differences were observed between converters and non-converters, but APOE e4 gene load and ADAS decline were, as expected, higher in converters. Also, 7 subjects initially classified as aMCI reverted to CU.

### 3.1. Group comparison of surface-based morphometry measures

#### 3.1.1. Longitudinal changes in cortical thickness

For detailed results please see Fig. 2 and Table 2. As anticipated, profound decreases of CTh were observed in both AD and aMCI in comparison to CU, most significantly within the bilateral temporal cortex and the temporal pole respectively and, in addition, within the frontal cortices and in the left insula. While in aMCI no other regions showed significant decreases of CTh during the observation period, additional decreases of cTH were found in AD subjects within medial frontal and parietal regions, including the precuneus and posterior cingulate cortex (PCC).

#### 3.1.2. Longitudinal changes in cortical complexity

For detailed results, please see Fig. 2 and Table 3. In comparison to CU, AD subjects yielded widespread decreases in FD, predominantly within the lateral and superior temporal cortex and adjacent occipital regions (left > right). Additional decreases were observed within medial temporal regions, posterior aspects of medial frontoparietal cortical regions including the precuneus and the PCC. Additional decreases were found within the central region and the dorsolateral aspects of the prefrontal cortex (PFC) (left > right). Increases of FD were found within the right anterior cingulate cortex.

In contrast, aMCI subjects only yielded subtle decreases of FD within posterior parts of the left superior temporal gyrus.

**Table 1**
Summary statistics.

| Group | AD (N = 96) | CU (N = 165) | aMCI (N = 211) | Total (N = 472) | p value |
|---|---|---|---|---|---|
| **Age** | | | | | 0.209 |
| Mean (SD) | 75.249 (7.387) | 76.036 (4.993) | 74.849 (7.041) | 75.345 (6.486) | |
| Range | 56.500–89.200 | 60.000–89.700 | 55.200–88.400 | 55.200–89.700 | |
| **Sex** | | | | | 0.002 |
| F | 46 (47.9%) | 81 (49.1%) | 69 (32.7%) | 196 (41.5%) | |
| M | 50 (52.1%) | 84 (50.9%) | 142 (67.3%) | 276 (58.5%) | |
| **Days to follow-up** | | | | | 0.489 |
| Mean (SD) | 743.896 (49.277) | 740.776 (30.519) | 739.014 (25.220) | 740.623 (33.182) | |
| **ADAS11-cog (baseline)** | | | | | < 0.001 |
| Mean (SD) | 18.563 (5.947) | 5.911 (2.845) | 11.366 (4.355) | 10.923 (6.260) | |
| **ADAS11-cog (follow-up)** | | | | | < 0.001 |
| Mean (SD) | 27.629 (11.320) | 5.833 (2.966) | 14.416 (7.730) | 14.103 (10.809) | |
| **Longitudinal Delta of ADAS11-cog** | | | | | < 0.001 |
| Mean (SD) | 9.067 (8.644) | −0.078 (3.087) | 3.049 (6.074) | 3.18 (6.755) | |
| **MMSE (baseline)** | | | | | < 0.001 |
| Mean (SD) | 23.219 (1.942) | 29.212 (0.923) | 27.104 (1.767) | 27.051 (2.661) | |
| **MMSE (follow-up)** | | | | | < 0.001 |
| Mean (SD) | 18.979 (5.555) | 29.104 (1.133) | 25.111 (4.19) | 25.253 (5.276) | |
| **Longitudinal Delta of MMSE** | | | | | < 0.001 |
| Mean (SD) | 4.24 (5.215) | 0.104 (1.246) | 1.981 (3.713) | 1.786 (3.799) | |
| **APOE** | | | | | < 0.001 |
| 2,2 | 0 (0.0%) | 2 (1.2%) | 0 (0.0%) | 2 (0.4%) | |
| 2,3 | 3 (3.1%) | 20 (12.1%) | 9 (4.3%) | 32 (6.8%) | |
| 2,4 | 3 (3.1%) | 2 (1.2%) | 8 (3.8%) | 13 (2.8%) | |
| 3,3 | 27 (28.1%) | 96 (58.2%) | 85 (40.3%) | 208 (44.1%) | |
| 3,4 | 41 (42.7%) | 40 (24.2%) | 83 (39.3%) | 164 (34.7%) | |
| 4,4 | 22 (22.9%) | 5 (3.0%) | 26 (12.3%) | 53 (11.2%) | |

AD Alzhimer's Disease.
CU Cognitively unimpaired.
aMCI amnestic mild cognitive impairment.
ADAS11-cog Alzheimer's Disease Assessment Scale-Cognitive Subscale.
MMSE Mini Mental Status Evaluation.

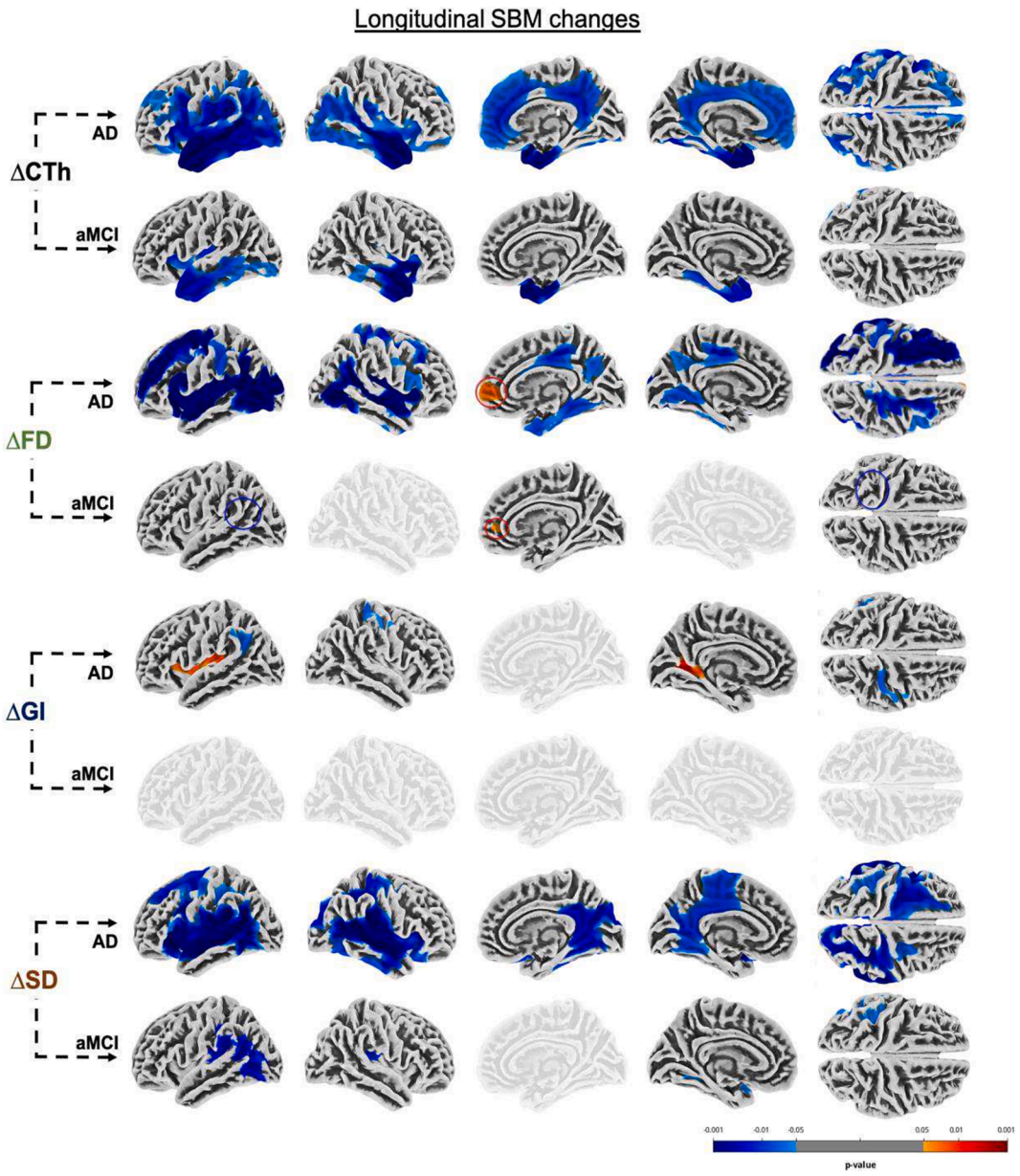


**Fig. 2.** Longitudinal changes of cortical thickness (CTh), cortical complexity (FD), gyrification index (GI) and sulcal depth (SD) in Alzheimer's Disease (AD) and amnestic mild cognitive impairment (aMCI) participants (all comparisons vs. cognitively unimpaired controls (CU)). n.s. not significant;

*3.1.3. Longitudinal changes of GI*

In AD compared to CU, longitudinal decreases of GI were observed within the left superior and middle temporal gyrus and the right post-central gyrus, whereas increases were noted within left medial occipital regions (i.e. lingual gyrus) and the left insular region. In MCI on the other hand, no differences in longitudinal GI changes were observed when compared to CU.

*3.1.4. Longitudinal changes of SD*

For detailed results please see Fig. 2 and Table 4. Compared to CU, AD showed extensive decreases of SD, most prominently within the bilateral insular-temporal region. Additional decreases were observed within the central region and the medial parietooccipital cortex, including parts of the posterior cingulate and the precuneus. In aMCI very similar yet less extent decreases were found, particularly within the left parietotemporal region (L > R).

*3.1.5. Converters vs. non-converters*

See Table S1 and Fig. S1) for detailed results. Post-hoc comparisons of subjects converting from aMCI to AD within the 2-year time frame in question with those who did not convert, showed extensive reductions of gray matter as measured by CTh (bilateral PFC, precuneus and temporal lobes, with emphasis on the right hemisphere) in converters. Gyrification was less developed for converters within the right frontal lobe. Analysis of cortical complexity and sulcal depth yielded no significant group differences.

*3.2. Associations of cognitive decline with longitudinal SBM changes*

Detailed results are provided in Fig. 3 and tables 2-5. No significant associations of cognitive decline (i.e. ADAS-Cog 11) with longitudinal changes of CTh were found in AD. In aMCI however, cTH decreases showed widespread associations with cognitive decline within AD-typical temporal, parietal and limbic regions. In contrast, longitudinal FD changes were associated with ADAS-Cog 11 in AD but not aMCI, with

**Table 2**
Longitudinal changes of cTH in AD and MCI in comparison to cognitively unimpaired controls and associations with cognitive decline.

| Brain Region | cluster size | p-value (FWE) | $MNI_{xyz}$ | |
|---|---|---|---|---|
| *Longitudinal changes in cTH(AD < CU):* | | | | |
| **L** | **Superior Temporal Gyrus** | **18,169** | **0.000** | **−42 14–26** |
| L | Middle Temporal Gyrus | | 0.000 | −53–14 −18 |
| L | Insula | | 0.000 | −41–30 20 |
| **R** | **Inferior Frontal Gyrus** | **12,644** | **0.000** | **41 15–26** |
| R | Sub-Gyral | | 0.000 | 47–5 −15 |
| R | Superior Temporal Gyrus | | 0.000 | 36 6–38 |
| *Longitudinal changes in cTH (MCI < CU):* | | | | |
| **R** | **Sub-Gyral Gray Matter (Temporal Lobe)** | **3821** | **0.000** | **44–10 −13** |
| R | Middle Temporal Gyrus | | 0.000 | 51 2–25 |
| R | Superior Temporal Gyrus | | 0.000 | 33 13–39 |
| **L** | **Superior Temporal Gyrus** | **3758** | **0.004** | **−44 16–29** |
| L | Insula | | 0.01 | −35–11 14 |
| L | Middle Temporal Gyrus | | 0.018 | −63–38 −8 |
| **L** | **Posterior Cingulate** | **37** | **0.048** | −4–58 14 |
| *Associations of longitudinal cTH changes with dADAS11 (AD):* **not significant** | | | | |
| *Associations of longitudinal changes in cTH with dADAS11 (MCI):* | | | | |
| **L** | **Supramarginal Gyrus** | **14,153** | **0.002** | **−58–47 22** |
| L | Superior Temporal Gyrus | | 0.002 | −49 13–19 |
| L | Superior Temporal Gyrus | | 0.002 | −57–0 −4 |
| **R** | **Superior Temporal Gyrus** | **10,285** | **0.005** | **55 8–16** |
| R | Middle Temporal Gyrus | | 0.008 | 54–33 −8 |
| R | Insula | | 0.01 | 39 13–9 |
| **R** | **Cingulate Gyrus** | **4677** | **0.011** | **16–28 41** |
| R | Cingulate Gyrus | | 0.016 | 6–38 34 |
| R | Cingulate Gyrus | | 0.018 | 10 40 23 |

MNI Montreal Neurological Institute.
CTh Cortical thickness.
dADAS11 Delta of Alzheimer's Disease Assessment Scale-Cognitive Subscale.
*Results are listed at a threshold of $p < 0.05$ FWE TFCE corrected;
Bold data indicate primary peak within a cluster; Non-bold data indicate secondary peaks.

associations being located within the right precuneus and adjacent central regions. In AD subjects, cognitive decline showed subtle associations with GI decreases within the right medial central region (i.e. paracentral lobule) and the left precentral gyrus. In aMCI, cognitive decline was associated with GI decreases in the insular/claustrum region and the medial PFC. For SD, subtle associations with ADAS11 were found with the right temporal cortex in AD (i.e. fusiform gyrus) and in aMCI within the left temporal cortex (i.e. superior temporal gyrus).

Additional post-hoc analyses showed a significant group*cognitive decline interaction for FD with stronger associations of cognitive decline with longitudinal FD reductions within the right medial postcentral

**Table 3**
Longitudinal changes of FD in AD and MCI in comparison to cognitively unimpaired controls and associations with cognitive decline.

| Brain Region | cluster size | p-value (FWE) | $MNI_{xyz}$ | |
|---|---|---|---|---|
| *Longitudinal changes in FD (AD < CU):* | | | | |
| **L** | **Claustrum** | **11,296** | **0.000** | **-37 -14 10** |
| L | Fusiform Gyrus | | 0.000 | -46 -73 -7 |
| L | Middle Occipital Gyrus | | 0.000 | -48 -80 7 |
| **R** | **Insula** | **3654** | **0.000** | **36 -20 14** |
| R | Superior Temporal Gyrus | | 0.000 | 54 7 -9 |
| R | Superior Temporal Gyrus | | 0.000 | 49 -19 -8 |
| **R** | **Precentral Gyrus** | **2379** | **0.002** | **30 -14 65** |
| R | Superior Frontal Gyrus | | 0.003 | 28 24 43 |
| R | Medial Frontal Gyrus | | 0.006 | 23 -11 55 |
| **R** | **Parahippocampal Gyrus** | **1639** | **0.009** | **19 -34 -9** |
| **L** | **Culmen** | **676** | **0.016** | **-10 -57 0** |
| **R** | **Precuneus** | **1657** | **0.017** | **11 -66 29** |
| R | Precuneus | | 0.017 | 5 -67 35 |
| R | Cingulate Gyrus | | 0.045 | 3 -48 27 |
| **R** | **Inferior Frontal Gyrus** | **462** | **0.026** | **47 11 20** |
| **L** | **Sub-Gyral** | **245** | **0.026** | **-43 -23 -24** |
| L | Parahippocampal Gyrus | | 0.027 | -39 -30 -25 |
| **L** | **Precuneus** | **1187** | **0.034** | **- 9 -56 34** |
| L | Precuneus | | 0.035 | -3-64 29 |
| L | Precuneus | | 0.038 | -4 -71 36 |
| **R** | **Medial Frontal Gyrus** | **125** | **0.043** | **26 49 8** |
| *Longitudinal changes in FD(AD > CU):* | | | | |
| **R** | **Anterior Cingulate** | **191** | **0.025** | **12 46 -1** |
| R | Medial Frontal Gyrus | | 0.025 | 8 55 6 |
| *Longitudinal changes in FD(MCI < CU):* | | | | |
| **L** | **Superior Temporal Gyrus** | **256** | **0.029** | -41 -56 22 |
| *Longitudinal changes in FD(MCI > CU):* | | | | |
| **R** | **Medial Frontal Gyrus** | **80** | **0.031** | **13 47 5** |
| *Associations of longitudinal FD changes with dADAS11 (AD):* | | | | |
| **R** | **Superior Parietal Lobe** | **1693** | **0.004** | **19 -41 68** |

(*continued on next page*)

**Table 3** (*continued*)

| Brain Region | cluster size | p-value (FWE) | $MNI_{xyz}$ | |
|---|---|---|---|---|
| | Superior Parietal Lobe | | 0.004 | 22 -49 71 |
| | Precuneus | | | 17 -53 60 |
| **R** | **Precentral Gyrus** | **724** | **0.039** | **25 -14 75** |
| | Precentral Gyrus | | | 26 -14 60 |
| | Middle Frontal Gyrus | | | 35 -5 48 |

MNI Montreal Neurological Institute.
FD Fractal dimension.
dADAS11 Delta of Alzheimer's Disease Assessment Scale-Cognitive Subscale.
*Results are listed at a threshold of $p < 0.05$ FWE TFCE corrected.
Bold data indicate primary peak within a cluster; Non-bold data indicate secondary peaks.

region and adjacent parts of the right superior parietal lobule and precuneus ($peak_{MNI}$: x = 18 y = -40 z = 67; k = 1693; $p_{TFCE} = 0.004$) and the right central region ($peak_{MNI}$: x = 24 y = -15 z = 74; k = 724; $p_{TFCE} = 0.039$), both clusters largely overlapping with the individual regression analysis. Nevertheless, for the other SBM measures (i.e. CTh, GI, SD) no significant group*cognitive decline interaction terms were observed.

## 4. Discussion

In our study, we investigated longitudinal changes of different surface based structural brain metrics in a well-characterized sample of participants with dementia due to AD, with its risk state aMCI and cognitively unimpaired healthy controls. Next to commonly used measures of cortical thickness, we applied additional metrics including cortical complexity (via fractal dimension; FD), gyrification index (GI) and sulcal depth (SD) in order to explore whether the respective longitudinal changes show different neuroanatomical patterns and relationship with cognitive decline in comparison to healthy controls.

Expectedly, we found marked decreases in CTh for AD and to a lesser degree in aMCI in comparison to CU, most significantly within the bilateral temporal cortices. In contrast, analyses of FD and GI yielded a more nuanced decline of the respective measures with some areas also showing increases in FD and GI. Overall changes in FD and GI were more pronounced in AD as compared to aMCI. Analyses of SD yielded widespread decreases, again more extent in AD. Interestingly, cognitive decline corresponded well with CTh declines in aMCI but not AD, whereas changes in FD were associated with cognitive decline in AD only and not aMCI. GI and SD were associated with cognitive decline in both, aMCI and AD. Expectedly, additional post-hoc analyses demonstrated stronger morphological changes in aMCI subjects converting to dementia stages, however most pronounced for CTh and less for GI and FD (but not SD).

We found cognitive decline to be associated with CTh reductions only in aMCI, but not in AD, while other SBM measures fared better, i.e. yielded significant associations. This suggests that the neurodegenerative process underlying the clinical presentation of AD encompasses, from a gross anatomical perspective, subtle changes in cortical complexity. Cortical folding, the process by which gyri and sulci are formed as part of embryonic development, is of decisive importance for phylogenetic and ontogenetic brain development. Cortical folding allows for a much larger number of neurons to be contained in the neurocranium while, by optimizing for space, respecting inherent size constraints (Fernández et al., 2016; Striedter et al., 2015). In addition to

**Table 4**
Longitudinal changes of SD in AD and MCI in comparison to cognitively unimpaired controls and associations with cognitive decline.

| Brain Region | cluster size | p-value (FWE) | $MNI_{xyz}$ | |
|---|---|---|---|---|
| *Longitudinal changes in SD (AD < CU):* | | | | |
| **L** | **Insula** | **13,481** | **0.000** | **-39 -27 21** |
| L | Superior Temporal Gyrus | | 0.000 | -35 -33 18 |
| L | Superior Temporal Gyrus | | 0.000 | -48 -31 5 |
| **R** | **Superior Temporal Gyrus** | **12,604** | **0.000** | **62 -2 -2** |
| R | Inferior Parietal Lobule | | 0.000 | 58 -23 23 |
| R | Claustrum | | 0.000 | 35 11 12 |
| **L** | **Precentral Gyrus** | **1698** | **0.010** | **-43 30 35** |
| L | Supramarginal Gyrus | | 0.016 | -38 -46 36 |
| L | Inferior Parietal Lobule | | 0.022 | -33 -39 49 |
| *Longitudinal changes in SD (MCI < CU):* | | | | |
| **L** | **Middle Temporal Gyrus** | **5420** | **0.01** | **-39 -58 18** |
| L | Superior Temporal Gyrus | | 0.01 | -52 -57 26 |
| L | Insula | | 0.01 | -42 -23 18 |
| **L** | **Supramarginal Gyrus** | **779** | **0.021** | **-37 -37 38** |
| L | Supramarginal Gyrus | | 0.026 | -44 -46 40 |
| L | Inferior Parietal Lobule | | 0.03 | -50 -34 39 |
| **R** | **Insula** | **720** | **0.038** | **37 -28 14** |
| R | Insula | | 0.038 | 34 -22 18 |
| R | Claustrum | | 0.039 | 40 -24 1 |
| *Associations of longitudinal SDchanges with dADAS11 (AD; neg.):* | | | | |
| **R** | **Fusiform Gyrus** | **76** | **0.049** | **51 -58 11** |
| R | Fusiform Gyrus | | 0.049 | 50 -45 7 |
| *Associations of longitudinal SD changes with dADAS11 (MCI; pos.):* | | | | |
| **L** | **Superior Temporal Gyrus** | **393** | **0.047** | **-52 -55 20** |
| L | Superior Temporal Gyrus | | 0.048 | -61 -48 21 |

MNI Montreal Neurological Institute.
SD Sulcal depth.
*Results are listed at a threshold of $p < 0.05$ FWE TFCE corrected;

Bold data indicate primary peak within a cluster; Non-bold data indicate secondary peaks.

conveying geometrical advantages, folding also directly influences brains' function by optimizing structural connectivity (Klyachko and Stevens, 2003). It therefore stands to reason that atrophy is more than the loss of matter, it is a loss of functionally relevant structure of matter. We suggest that reduction of cortical complexity amounts to deoptimization, explaining its independent association with cognitive decline. Strikingly, we observed regionally circumscribed increases in all measures but CTh over time. While neurodegeneration is more likely to result in less cortical complexity, it is conceivable that, in some cases, it might deepen and widen sulci and emphasize the morphological aspect of cortical folding.

Several limitations of our study need to be acknowledged. The retrospective character and lack of real-world data (the ADNI's acquisition of imaging and behavioral data is done under carefully controlled and optimized conditions) limits our study's transferability into clinical practice. We also need to acknowledge the risk of type I errors due to the sheer number of comparisons we carried out. In our study, only two timepoints were analyzed. Future studies might shed additional light on the temporal dynamics of brain morphological changes by incorporating additional timepoints and other brain structural parameters such as white matter volume changes and whether incorporating measures of cortical geometry might enhance diagnosis and progression tracking of AD. Also, it might have been worth investigating how functional connectivity is affected by chsanges in cortical complexity. While the ADNI offers functional task-free MRI data, analyzing this aspect was beyond the scope of our study.

In summary, our comparison of different SBM measures in AD and aMCI subjects over a 2-year period of time found more complex measures to be associated with cognitive decline in AD while the simplest, CTh, was not, suggesting a "burn-out" effect in manifest disease, where further decline in function is not necessarily reflected in gross loss of gray-matter volume. Overall, our results suggest a sequence of structural deterioration in disease progression with reduction in CTh dominating

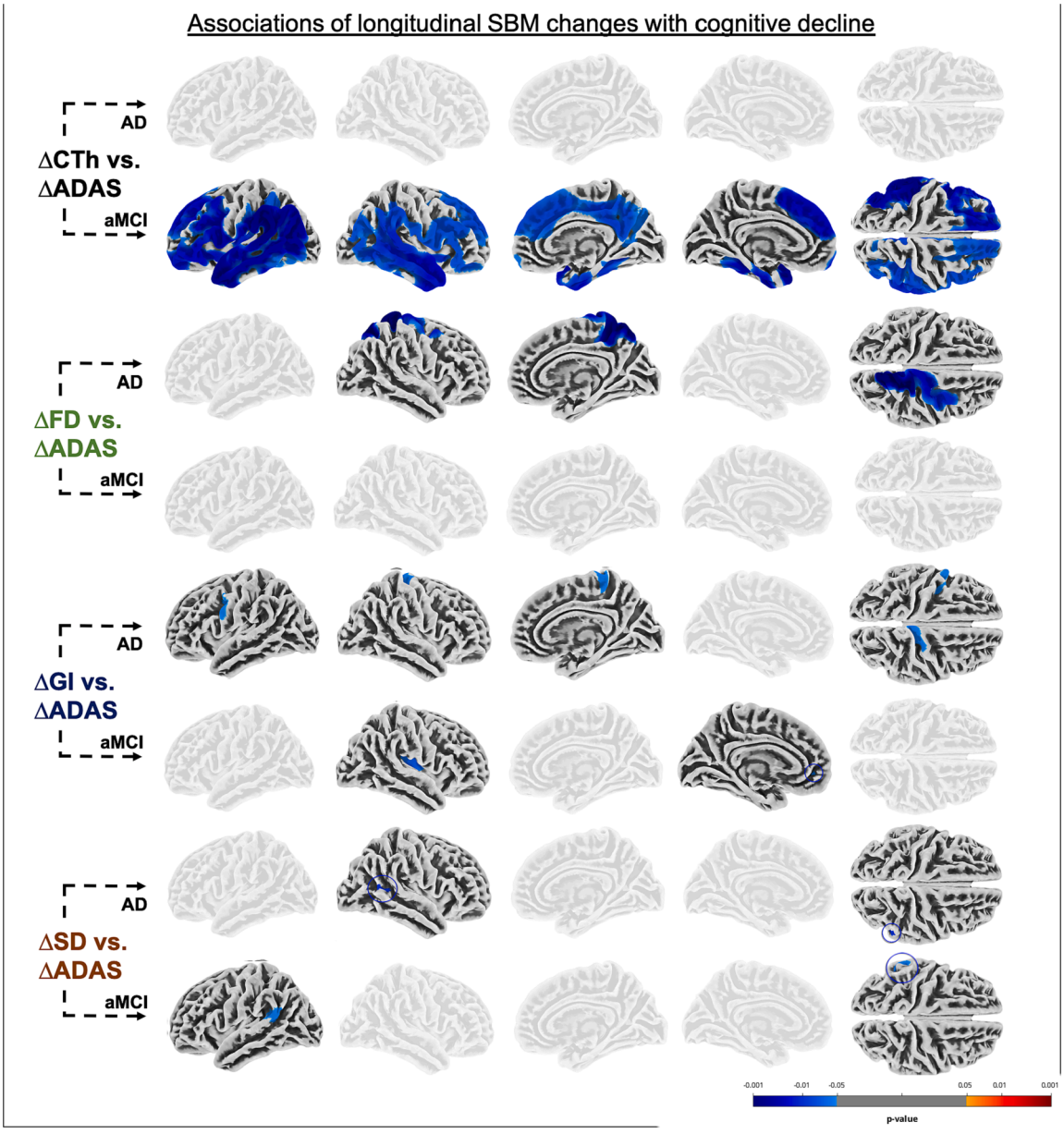


**Fig. 3.** Direct associations of longitudinal decreases of cortical thickness (CTh), cortical complexity (FD), gyrification index (GI) and sulcal depth (SD) in Alzheimer's Disease AD and amnestic mild cognitive impairment (aMCI) participants with longitudinal cognitive decline (via ADAS-Cog 11). n.s. not significant.

**Table 5**
Longitudinal changes of GI in AD and MCI in comparison to cognitively unimpaired controls and associations with cognitive decline.

| Brain Region | cluster size | p-value (FWE) | $MNI_{xyz}$ | |
|---|---|---|---|---|
| *Longitudinal changes in GI (AD < CU):* | | | | |
| **L** | **Superior Temporal Gyrus** | **682** | **0.012** | **-44 -58 26** |
| L | Superior Temporal Gyrus | | 0.018 | -49 -53 33 |
| **R** | **Postcentral Gyrus** | **517** | **0.023** | **38 -35 63** |
| R | Postcentral Gyrus | | 0.037 | 46 -22 61 |
| **L** | **MiddleTemporal Gyrus** | **76** | **0.046** | **-57 -62 7** |
| *Longitudinal changes in GI (AD > CU):* | | | | |
| **L** | **Lingual Gyrus** | **447** | **0.011** | **-24 -62 6** |
| **L** | **Insula** | **703** | **0.029** | **-32 -27 10** |
| *Associations of longitudinal GI changes with dADAS11 (AD; pos.):* | | | | |
| **R** | **Paracentral Lobule** | **401** | **0.04** | **4 -37 58** |
| **L** | **Precentral Gyrus** | **241** | **0.043** | **-57 7 28** |
| L | Precentral Gyrus | | 0.046 | -46 -1 33 |
| L | Precentral Gyrus | | 0.049 | -44 4 48 |
| *Associations of longitudinal GI changes with dADAS11 (MCI; pos.):* | | | | |
| **R** | **Claustrum** | **546** | **0.024** | **35 -12 13** |
| **L** | **Anterior Cingulate** | **8** | **0.05** | **-13 46 -2** |

MNI Montreal Neurological Institute.
GI Gyrification index.
*Results are listed at a threshold of $p < 0.05$ FWE TFCE corrected;
Bold data indicate primary peak within a cluster; Non-bold data indicate secondary peaks.

early stages followed by additional changes in cortical complexity in later stages. Clinically, combining volumetric and SBM measures can increase the sensitivity of diagnosis based on neuroimaging markers and aid disease tracking especially in advanced disease.

## Declaration of Competing Interest

The authors declare that they have no known competing financial interests or personal relationships that could have appeared to influence the work reported in this paper.

## Data availability

Data will be made available on request.

## Acknowledgements

Data collection and sharing for this project was funded by the Alzheimer's Disease Neuroimaging Initiative (ADNI) (National Institutes of Health Grant U01 AG024904) and DOD ADNI (Department of Defense award number W81XWH-12-2-0012). ADNI is funded by the National Institute on Aging, the National Institute of Biomedical Imaging and Bioengineering, and through generous contributions from the following: AbbVie, Alzheimer's Association; Alzheimer's Drug Discovery Foundation; Araclon Biotech; BioClinica, Inc.; Biogen; Bristol-Myers Squibb Company; CereSpir, Inc.; Cogstate; Eisai Inc.; Elan Pharmaceuticals, Inc.; Eli Lilly and Company; EuroImmun; F. Hoffmann-La Roche Ltd and its affiliated company Genentech, Inc.; Fujirebio; GE Healthcare; IXICO Ltd.;Janssen Alzheimer Immunotherapy Research & Development, LLC.; Johnson & Johnson Pharmaceutical Research & Development LLC.; Lumosity; Lundbeck; Merck & Co., Inc. ;Meso Scale Diagnostics, LLC.; NeuroRx Research; Neurotrack Technologies; Novartis Pharmaceuticals Corporation; Pfizer Inc.; Piramal Imaging; Servier; Takeda Pharmaceutical Company; and Transition Therapeutics. The Canadian Institutes of Health Research is providing funds to support ADNI clinical sites in Canada. Private sector contributions are facilitated by the Foundation for the National Institutes of Health (www.fnih.org). The grantee organization is the Northern California Institute for Research and Education, and the study is coordinated by the Alzheimer's Therapeutic Research Institute at the University of Southern California. ADNI data are disseminated by the Laboratory for Neuro Imaging at the University of Southern California.

## Appendix A. Supplementary data

Supplementary data to this article can be found online at https://doi.org/10.1016/j.nicl.2023.103371.

## References

Acosta, O., Bourgeat, P., Zuluaga, M.A., Fripp, J., Salvado, O., Ourselin, S., 2009. Automated voxel-based 3D cortical thickness measurement in a combined Lagrangian-Eulerian PDE approach using partial volume maps. Med. Image Anal. 13, 730–743. https://doi.org/10.1016/j.media.2009.07.003.

Baxter, L.C., Sparks, D.L., Johnson, S.C., Lenoski, B., Lopez, J.E., Connor, D.J., Sabbagh, M.N., 2006. Relationship of cognitive measures and gray and white matter in Alzheimer's disease. J. Alzheimers Dis. 9, 253–260. https://doi.org/10.3233/JAD-2006-9304.

Bejanin, A., Schonhaut, D.R., La Joie, R., Kramer, J.H., Baker, S.L., Sosa, N., Ayakta, N., Cantwell, A., Janabi, M., Lauriola, M., O'Neil, J.P., Gorno-Tempini, M.L., Miller, Z. A., Rosen, H.J., Miller, B.L., Jagust, W.J., Rabinovici, G.D., 2017. Tau pathology and neurodegeneration contribute to cognitive impairment in Alzheimer's disease. Brain 140, 3286–3300. https://doi.org/10.1093/brain/awx243.

Clarkson, M.J., Cardoso, M.J., Ridgway, G.R., Modat, M., Leung, K.K., Rohrer, J.D., Fox, N.C., Ourselin, S., 2011. A comparison of voxel and surface based cortical thickness estimation methods. NeuroImage 57, 856–865. https://doi.org/10.1016/j.neuroimage.2011.05.053.

Dahnke, R., Yotter, R.A., Gaser, C., 2013. Cortical thickness and central surface estimation. NeuroImage 65, 336–348. https://doi.org/10.1016/j.neuroimage.2012.09.050.

Dale, A.M., Fischl, B., Sereno, M.I., 1999. Cortical Surface-Based Analysis. NeuroImage 9, 179–194. https://doi.org/10.1006/nimg.1998.0395.

de Leon, M.J., Convit, A., DeSanti, S., Bobinski, M., George, A.E., Wisniewski, H.M., Rusinek, H., Carroll, R., Louis, L.A.S., 1997. Contribution of Structural Neuroimaging to the Early Diagnosis of Alzheimer's Disease. Int. Psychogeriatr. 9, 183–190. https://doi.org/10.1017/S1041610297004900.

Dong, Q., Zhang, W., Stonnington, C.M., Wu, J., Gutman, B.A., Chen, K., Su, Y., Baxter, L. C., Thompson, P.M., Reiman, E.M., Caselli, R.J., Wang, Y., 2020. Applying surface-based morphometry to study ventricular abnormalities of cognitively unimpaired subjects prior to clinically significant memory decline. NeuroImage Clin. 27, 102338 https://doi.org/10.1016/j.nicl.2020.102338.

Dubois, B., Feldman, H.H., Jacova, C., Cummings, J.L., DeKosky, S.T., Barberger-Gateau, P., Delacourte, A., Frisoni, G., Fox, N.C., Galasko, D., Gauthier, S., Hampel, H., Jicha, G.A., Meguro, K., O'Brien, J., Pasquier, F., Robert, P., Rossor, M., Salloway, S., Sarazin, M., de Souza, L.C., Stern, Y., Visser, P.J., Scheltens, P., 2010. Revising the definition of Alzheimer's disease: a new lexicon. Lancet Neurol. 9, 1118–1127. https://doi.org/10.1016/S1474-4422(10)70223-4.

Eklund, A., Nichols, T.E., Knutsson, H., 2016. Cluster failure: Why fMRI inferences for spatial extent have inflated false-positive rates. Proc. Natl. Acad. Sci. U. S. A. 113, 7900–7905. https://doi.org/10.1073/pnas.1602413113.

Femminella, G., Thayanandan, T., Calsolaro, V., Komici, K., Rengo, G., Corbi, G., Ferrara, N., 2018. Imaging and Molecular Mechanisms of Alzheimer's Disease: A Review. Int. J. Mol. Sci. 19, 3702. https://doi.org/10.3390/ijms19123702.

Fernández, V., Llinares-Benadero, C., Borrell, V., 2016. Cerebral cortex expansion and folding: what have we learned? EMBO J 35, 1021–1044. https://doi.org/10.15252/embj.201593701.

Fischl, B., Dale, A.M., 2000. Measuring the thickness of the human cerebral cortex from magnetic resonance images. Proc. Natl. Acad. Sci. 97, 11050–11055. https://doi.org/10.1073/pnas.200033797.

Fischl, B., Sereno, M.I., Dale, A.M., 1999. Cortical Surface-Based Analysis. NeuroImage 9, 195–207. https://doi.org/10.1006/nimg.1998.0396.

Folstein, M.F., Folstein, S.E., McHugh, P.R., 1975. Mini-mental state. J. Psychiatr. Res. 12, 189–198. https://doi.org/10.1016/0022-3956(75)90026-6.

Gordon, B.A., Blazey, T.M., Su, Y., Hari-Raj, A., Dincer, A., Flores, S., Christensen, J., McDade, E., Wang, G., Xiong, C., Cairns, N.J., Hassenstab, J., Marcus, D.S., Fagan, A. M., Jack, C.R., Hornbeck, R.C., Paumier, K.L., Ances, B.M., Berman, S.B., Brickman, A.M., Cash, D.M., Chhatwal, J.P., Correia, S., Förster, S., Fox, N.C., Graff-Radford, N.R., la Fougère, C., Levin, J., Masters, C.L., Rossor, M.N., Salloway, S., Saykin, A.J., Schofield, P.R., Thompson, P.M., Weiner, M.M., Holtzman, D.M., Raichle, M.E., Morris, J.C., Bateman, R.J., Benzinger, T.L.S., 2018. Spatial patterns of neuroimaging biomarker change in individuals from families with autosomal dominant Alzheimer's disease: a longitudinal study. Lancet Neurol. 17, 241–250. https://doi.org/10.1016/S1474-4422(18)30028-0.

Ha, T.H., Yoon, U., Lee, K.J., Shin, Y.W., Lee, J.-M., Kim, I.Y., Ha, K.S., Kim, S.I., Kwon, J. S., 2005. Fractal dimension of cerebral cortical surface in schizophrenia and obsessive–compulsive disorder. Neurosci. Lett. 384, 172–176. https://doi.org/10.1016/j.neulet.2005.04.078.

Hughes, C.P., Berg, L., Danziger, W., Coben, L.A., Martin, R.L., 1982. A New Clinical Scale for the Staging of Dementia. Br. J. Psychiatry 140, 566–572. https://doi.org/10.1192/bjp.140.6.566.

Karas, G.B., Scheltens, P., Rombouts, S., a. R.B., Visser, P.J., van Schijndel, R.A., Fox, N. C., Barkhof, F.,, 2004. Global and local gray matter loss in mild cognitive impairment and Alzheimer's disease. NeuroImage 23, 708–716. https://doi.org/10.1016/j.neuroimage.2004.07.006.

King, R.D., George, A.T., Jeon, T., Hynan, L.S., Youn, T.S., Kennedy, D.N., Dickerson, B., 2009. Characterization of Atrophic Changes in the Cerebral Cortex Using Fractal Dimensional Analysis. Brain Imaging Behav. 3, 154–166. https://doi.org/10.1007/s11682-008-9057-9.

King, R.D., Brown, B., Hwang, M., Jeon, T., George, A.T., 2010. Fractal dimension analysis of the cortical ribbon in mild Alzheimer's disease. NeuroImage 53, 471–479. https://doi.org/10.1016/j.neuroimage.2010.06.050.

Klyachko, V.A., Stevens, C.F., 2003. Connectivity optimization and the positioning of cortical areas. Proc. Natl. Acad. Sci. 100, 7937–7941. https://doi.org/10.1073/pnas.0932745100.

Lerch, J.P., Evans, A.C., 2005. Cortical thickness analysis examined through power analysis and a population simulation. NeuroImage 24, 163–173. https://doi.org/10.1016/j.neuroimage.2004.07.045.

Li, K., Qu, H., Ma, M., Xia, C., Cai, M., Han, F., Zhang, Q., Gu, X., Ma, Q., 2022. Correlation Between Brain Structure Atrophy and Plasma Amyloid-β and Phosphorylated Tau in Patients With Alzheimer's Disease and Amnestic Mild Cognitive Impairment Explored by Surface-Based Morphometry. Front. Aging Neurosci. 14, 816043 https://doi.org/10.3389/fnagi.2022.816043.

Libero, L.E., Schaer, M., Li, D.D., Amaral, D.G., Nordahl, C.W., 2019. A Longitudinal Study of Local Gyrification Index in Young Boys With Autism Spectrum Disorder. Cereb. Cortex 29, 2575–2587. https://doi.org/10.1093/cercor/bhy126.

Luders, E., Thompson, P.M., Narr, K.L., Toga, A.W., Jancke, L., Gaser, C., 2006. A curvature-based approach to estimate local gyrification on the cortical surface. NeuroImage 29, 1224–1230. https://doi.org/10.1016/j.neuroimage.2005.08.049.

Matsuda, Y., Ohi, K., 2018. Cortical gyrification in schizophrenia: current perspectives. Neuropsychiatr. Dis. Treat. 14, 1861–1869. https://doi.org/10.2147/NDT.S145273.

McKhann, G.M., Knopman, D.S., Chertkow, H., Hyman, B.T., Jack, C.R., Kawas, C.H., Klunk, W.E., Koroshetz, W.J., Manly, J.J., Mayeux, R., Mohs, R.C., Morris, J.C., Rossor, M.N., Scheltens, P., Carrillo, M.C., Thies, B., Weintraub, S., Phelps, C.H., 2011. The diagnosis of dementia due to Alzheimer's disease: Recommendations from the National Institute on Aging-Alzheimer's Association workgroups on diagnostic guidelines for Alzheimer's disease. Alzheimers Dement. 7, 263–269. https://doi.org/10.1016/j.jalz.2011.03.005.

Nicastro, N., Malpetti, M., Cope, T.E., Bevan-Jones, W.R., Mak, E., Passamonti, L., Rowe, J.B., O'Brien, J.T., 2020. Cortical Complexity Analyses and Their Cognitive Correlate in Alzheimer's Disease and Frontotemporal Dementia. J. Alzheimers Dis. JAD 76, 331–340. https://doi.org/10.3233/JAD-200246.

Park, M., Moon, W.-J., 2016. Structural MR Imaging in the Diagnosis of Alzheimer's Disease and Other Neurodegenerative Dementia: Current Imaging Approach and Future Perspectives. Korean J. Radiol. 17, 827. https://doi.org/10.3348/kjr.2016.17.6.827.

Petersen, R.C., Aisen, P.S., Beckett, L.A., Donohue, M.C., Gamst, A.C., Harvey, D.J., Jack, C.R., Jagust, W.J., Shaw, L.M., Toga, A.W., Trojanowski, J.Q., Weiner, M.W., 2010. Alzheimer's Disease Neuroimaging Initiative (ADNI): Clinical characterization. Neurology 74, 201–209. https://doi.org/10.1212/WNL.0b013e3181cb3e25.

Prince, M., Albanese, E., Guerchet, M., Prina, M., 2014. World Alzheimer Report 2014: Dementia and Risk Reduction: An Analysis of Protective and Modifiable Factors.

Qin, Y., Cui, J., Ge, X., Tian, Y., Han, H., Fan, Z., Liu, L., Luo, Y., Yu, H., 2022. Hierarchical multi-class Alzheimer's disease diagnostic framework using imaging and clinical features. Front. Aging Neurosci. 14, 935055 https://doi.org/10.3389/fnagi.2022.935055.

R Core Team, 2020. R: A Language and Environment for Statistical Computing. R Foundation for Statistical Computing, Vienna, Austria.

Risacher, S.L., Anderson, W.H., Charil, A., Castelluccio, P.F., Shcherbinin, S., Saykin, A. J., Schwarz, A.J., For the Alzheimer's Disease Neuroimaging Initiative,, 2017. Alzheimer disease brain atrophy subtypes are associated with cognition and rate of decline. Neurology 89, 2176–2186. https://doi.org/10.1212/WNL.0000000000004670.

Rosen, W.G., Mohs, R.C., Davis, K.L., 1984. A new rating scale for Alzheimer's disease. Am J Psychiatry 141, 1356–1364. https://doi.org/10.1176/ajp.141.11.1356.

Ruiz de Miras, J., Costumero, V., Belloch, V., Escudero, J., Ávila, C., Sepulcre, J., 2017. Complexity analysis of cortical surface detects changes in future Alzheimer's disease converters: Cortical Surface Changes in Alzheimer's Disease. Hum. Brain Mapp. 38, 5905–5918. https://doi.org/10.1002/hbm.23773.

Schaer, M., Ottet, M.-C., Scariati, E., Dukes, D., Franchini, M., Eliez, S., Glaser, B., 2013. Decreased frontal gyrification correlates with altered connectivity in children with autism. Front. Hum. Neurosci. 7 https://doi.org/10.3389/fnhum.2013.00750.

Schroeter, M.L., Stein, T., Maslowski, N., Neumann, J., 2009. Neural correlates of Alzheimer's disease and mild cognitive impairment: A systematic and quantitative meta-analysis involving 1351 patients. NeuroImage 47, 1196–1206. https://doi.org/10.1016/j.neuroimage.2009.05.037.

Smith, S., Nichols, T., 2009. Threshold-free cluster enhancement: Addressing problems of smoothing, threshold dependence and localisation in cluster inference. NeuroImage 44, 83–98. https://doi.org/10.1016/j.neuroimage.2008.03.061.

Sterling, N.W., Wang, M., Zhang, L., Lee, E.-Y., Du, G., Lewis, M.M., Styner, M., Huang, X., 2016. Stage-dependent loss of cortical gyrification as Parkinson disease "unfolds". Neurology 86, 1143–1151. https://doi.org/10.1212/WNL.0000000000002492.

Striedter, G.F., Srinivasan, S., Monuki, E.S., 2015. Cortical Folding: When, Where, How, and Why? Annu. Rev. Neurosci. 38, 291–307. https://doi.org/10.1146/annurev-neuro-071714-034128.

Whitwell, J.L., Dickson, D.W., Murray, M.E., Weigand, S.D., Tosakulwong, N., Senjem, M.L., Knopman, D.S., Boeve, B.F., Parisi, J.E., Petersen, R.C., Jack, C.R., Josephs, K.A., 2012. Neuroimaging correlates of pathologically defined subtypes of Alzheimer's disease: a case-control study. Lancet Neurol. 11, 868–877. https://doi.org/10.1016/S1474-4422(12)70200-4.

Wu, Z., Peng, Y., Hong, M., Zhang, Y., 2021. Gray Matter Deterioration Pattern During Alzheimer's Disease Progression: A Regions-of-Interest Based Surface Morphometry Study. Front. Aging Neurosci. 13, 593898 https://doi.org/10.3389/fnagi.2021.593898.

Wyman, B.T., 2013. Standardization of analysis sets for reporting results from ADNI MRI data 6.

Gaser, C., Dahnke, R., n.d. CAT12 Manual 66.

Yotter, R.A., Nenadic, I., Ziegler, G., Thompson, P.M., Gaser, C., 2011. Local cortical surface complexity maps from spherical harmonic reconstructions. NeuroImage 56, 961–973. https://doi.org/10.1016/j.neuroimage.2011.02.007.

Zhang, Y., Liu, S., 2018. Analysis of structural brain MRI and multi-parameter classification for Alzheimer's disease. Biomed. Eng. Biomed. Tech. 63, 427–437. https://doi.org/10.1515/bmt-2016-0239.

Zilles, K., Armstrong, E., Schleicher, A., Kretschmann, H.-J., 1988. The human pattern of gyrification in the cerebral cortex. Anat. Embryol. (Berl.) 179, 173–179. https://doi.org/10.1007/BF00304699.